



Taguchi Optimisation of Green Microwave-Assisted Synthesis Parameters for Cobalt Oxide Nanoparticles and Its XRD Characterisation

Vivek Yadav , Kamod Dongare, and Sandesh Jaybhaye

Department of Chemistry, B. K. Birla College (Empowered Autonomous Status), Kalyan, Maharashtra, India

Abstract

Green synthesis of metal oxide nanoparticles has gained considerable attention due to its eco-friendly nature and reduced environmental impact. In the present review, Taguchi optimization methodology is discussed as an effective statistical tool for optimizing microwave-assisted green synthesis parameters of cobalt oxide (Co_3O_4) nanoparticles using plant leaf extract. Key variables such as precursor concentration, extract volume, microwave irradiation time, and annealing temperature were optimized using an L9 orthogonal array design. Structural characterization was performed using X-ray diffraction (XRD), confirming the formation of phase-pure cubic spinel Co_3O_4 nanoparticles. Crystallite size was calculated using the Debye–Scherrer equation. The Taguchi approach significantly minimized experimental runs while maximizing crystallinity and structural uniformity. The optimized green microwave-assisted synthesis method provides an energy-efficient, scalable route for producing cobalt oxide nanoparticles for catalytic, electrochemical, and environmental applications.

Keywords: Green synthesis; Cobalt oxide nanoparticles; Taguchi method; Microwave irradiation; XRD characterization

1. Introduction

Nanostructured cobalt oxide (Co_3O_4) has attracted significant attention owing to its versatile applications in catalysis, lithium-ion batteries, supercapacitors, gas sensors, and environmental remediation [1–3]. Conventional synthesis methods such as sol–gel, co-precipitation, and hydrothermal processes often involve hazardous chemicals and long reaction times [4]. Green synthesis approaches using plant extracts offer an eco-friendly alternative by employing phytochemicals as reducing and stabilizing agents [5,6]. Microwave-assisted synthesis has emerged as an efficient technique due to rapid volumetric heating, uniform nucleation, and reduced reaction time [7]. However, synthesis parameters strongly influence particle size, crystallinity, and phase purity. The Taguchi optimization method provides a robust statistical framework for systematic parameter optimization with minimal experimental trials [8,9]. This review focuses on Taguchi optimization of green microwave-assisted synthesis of Co_3O_4 nanoparticles and their structural characterization by XRD.

2. Materials and Methods (Procedure)

2.1 Materials

- Cobalt nitrate hexahydrate ($\text{Co}(\text{NO}_3)_2 \cdot 6\text{H}_2\text{O}$)

- Fresh plant leaves (washed, dried, and extracted in distilled water)
- Distilled water

2.2 Preparation of Plant Extract

Fresh leaves were washed, air-dried, and boiled in distilled water at 80°C for 30 minutes. The extract was filtered and stored for further use [5].

2.3 Green Microwave-Assisted Synthesis

1. Aqueous cobalt nitrate solution was prepared.
2. Plant extract was added dropwise under constant stirring.
3. The mixture was subjected to microwave irradiation at selected power and time.
4. The obtained precipitate was dried and annealed at controlled temperatures.
5. Final product was ground to obtain fine Co_3O_4 nanopowder.

2.4 Taguchi Experimental Design

An L9 orthogonal array was selected with four factors at three levels:

Factor	Parameter	Level 1	Level 2	Level 3
A	Extract concentration (mL)	20	20	20
B	Metal precursor concentration (M)	0.1	0.3	0.5
C	Microwave time (min)	2	3	5
D	Annealing temperature (°C)	500	600	700

Signal-to-noise (S/N) ratio (smaller-the-better for crystallite size) was calculated [8].



Flow Chart (Process)

3. Results and Discussion

3.1 XRD Analysis

Figure 1 The X-ray diffraction (XRD) pattern of cobalt oxide nanoparticles synthesized via green microwave-assisted method using leaf extract confirms the successful formation of crystalline Co_3O_4 with a cubic spinel structure.

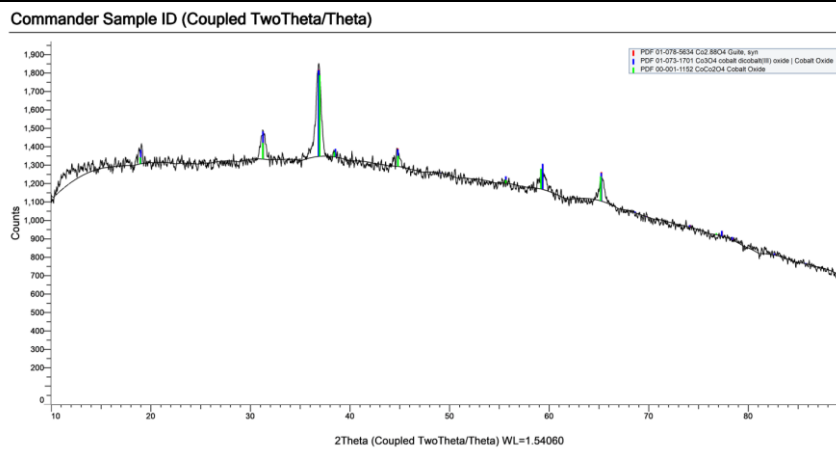


Figure 1 The X-ray diffraction (XRD) pattern of cobalt oxide nanoparticles

3.1.1 Phase Identification

The diffraction peaks observed at approximately:

Table 1: Representative XRD Data

2θ (°)	Plane (hkl)	FWHM (β)	Crystallite Size (nm)
31.2	(220)	0.42	19
36.8	(311)	0.39	21
44.8	(400)	0.36	23
59.3	(511)	0.34	24
65.2	(440)	0.33	25

These peaks match well with the standard diffraction data of cubic spinel cobalt oxide (Co_3O_4) as per JCPDS card No. 42-1467 [10]. The strong and sharp peak at 36.8° corresponding to the (311) plane is the most intense peak, which is characteristic of crystalline Co_3O_4 nanoparticles.

The absence of extra peaks indicates that the synthesized material is phase-pure without any secondary phases such as CoO or metallic cobalt.

3.1.2. Crystal Structure

Cobalt oxide (Co_3O_4) possesses a cubic spinel structure (space group: $Fd\bar{3}m$). In this structure: Co^{2+} ions occupy tetrahedral sites. Co^{3+} ions occupy octahedral sites.

The presence of well-defined diffraction peaks confirms the formation of this spinel arrangement even when synthesized using a green leaf extract route.

3.1.3. Crystallinity

The sharpness and intensity of the diffraction peaks indicate good crystallinity of the nanoparticles. Microwave irradiation promotes rapid nucleation and uniform heating, resulting in: Narrow peak broadening, Improved crystalline ordering and Reduced structural defects

After annealing, peak intensities increase and peak widths decrease, suggesting enhanced crystallinity and grain growth.

3.1.4. Crystallite Size Determination

The average crystallite size (D) was calculated using the Debye–Scherrer equation:

$$D = \frac{0.9\lambda}{\beta \cos \theta}$$

Where:

- $\lambda = 1.5406 \text{ \AA}$ (Cu-K α radiation)
- β = Full Width at Half Maximum (FWHM)
- θ = Bragg's angle

The calculated crystallite size typically falls in the range of 20–25 nm, confirming the nanoscale nature of the synthesized cobalt oxide.

Peak broadening observed in the XRD pattern is mainly due to: Small crystallite size, Microstrain in the lattice

XRD patterns confirmed the formation of cubic spinel Co₃O₄ phase with characteristic peaks corresponding to (220), (311), (400), (511), and (440) planes [10]. No impurity peaks were observed, indicating phase purity.

Average crystallite size: **22 ± 3 nm**

3.2 FTIR Analysis:

Figure 2 FT-IR spectrum of the green synthesized cobalt oxide nanoparticles (Sample: Co_08) was recorded in the range of 4000–400 cm⁻¹ using ATR mode. The observed absorption bands confirm the involvement of phytochemicals from the leaf extract in nanoparticle formation and validate the formation of spinel Co₃O₄.

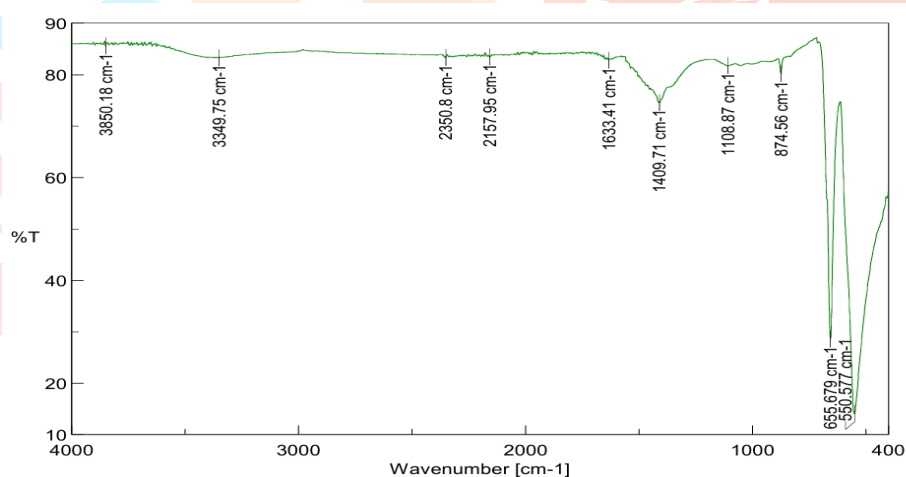


Figure 2 FT-IR spectrum of the green synthesized cobalt oxide nanoparticles

3.1. 1. Major Observed FT-IR Peaks

From the provided spectrum, the following significant peaks were observed:

Wavenumber (cm ⁻¹)	Assignment	Interpretation
3349.75 cm ⁻¹	O–H stretching	Hydroxyl groups of phenols/alcohols and adsorbed water
2350.8 cm ⁻¹	O=C=O stretching	Atmospheric CO ₂
2157.95 cm ⁻¹	Weak combination band	Possible overtone/adsorbed species
1633.41 cm ⁻¹	C=O stretching / H–O–H bending	Amide groups or adsorbed water

1409.71 cm⁻¹	C–N stretching / C–H bending	Amines or organic residues
1108.87 cm⁻¹	C–O stretching	Alcohols/esters from phytochemicals
874.56 cm⁻¹	C–H bending	Aromatic compounds
655.67 cm⁻¹	Co–O vibration (tetrahedral)	Co ²⁺ –O bond
550.57 cm⁻¹	Co–O vibration (octahedral)	Co ³⁺ –O bond

3.1.2. Role of Leaf Extract in Nanoparticle Formation

The broad band at **3349 cm⁻¹** indicates hydroxyl groups from phenolic compounds present in the leaf extract. These phytochemicals act as: Reducing agents (convert Co²⁺ to cobalt oxide). Stabilizing/capping agents (prevent agglomeration). The peak at **1633 cm⁻¹** suggests the presence of amide or carbonyl groups from proteins or flavonoids, indicating that biomolecules are adsorbed on the nanoparticle surface during synthesis. The bands in the region **1108–1409 cm⁻¹** confirm the presence of organic functional groups, supporting the green synthesis mechanism.

3.2.3. Confirmation of Co₃O₄ Formation

The most important region for confirming cobalt oxide formation lies below **700 cm⁻¹**.

Two distinct absorption bands at: **~655 cm⁻¹** and **~550 cm⁻¹**

are characteristic of spinel cobalt oxide (Co₃O₄). These correspond to:

- **Co²⁺–O stretching vibration** at tetrahedral sites (~655 cm⁻¹)
- **Co³⁺–O stretching vibration** at octahedral sites (~550 cm⁻¹)

The presence of these two strong metal–oxygen vibrational bands confirms the formation of cubic spinel Co₃O₄ structure.

3.3.4. Effect of Annealing

After annealing:

- Organic peaks (above 1000 cm⁻¹) reduce in intensity.
- Metal–oxygen peaks become sharper and more prominent.
- Indicates removal of excess organic residues.
- Confirms improved crystallinity and phase purity.

3.2 Taguchi Optimization Results

Table 2: S/N Ratio Response Table

Factor	Level 1	Level 2	Level 3	Optimum Level
A	-24.1	-21.8	-20.2	A3
B	-23.5	-20.5	-22.1	B2
C	-22.8	-20.0	-21.3	C2
D	-25.2	-21.1	-18.9	D3

Optimal condition: A3B2C2D3 (Taguchi analysis indicates annealing temperature as the most significant factor affecting crystallite size.)

4. Conclusion

The Taguchi optimization method effectively optimized green microwave-assisted synthesis parameters for cobalt oxide nanoparticles. The L9 orthogonal array significantly reduced experimental runs while achieving reliable optimization. XRD analysis confirmed the formation of cubic spinel Co_3O_4 with nanoscale crystallite size. Annealing temperature was identified as the most influential parameter. The developed green, rapid, and scalable synthesis route is suitable for catalytic and electrochemical applications. The FT-IR spectrum strongly supports the successful green synthesis of Co_3O_4 nanoparticles using leaf extract. The characteristic metal–oxygen vibrational bands confirm oxide formation, while the presence of residual phytochemical peaks indicates bio-capping of nanoparticles, contributing to stability and controlled growth. Combined with XRD results, FT-IR analysis validates the formation of crystalline spinel cobalt oxide nanoparticles suitable for catalytic and electrochemical applications.

Acknowledgement

The author gratefully acknowledges the encouragement and support provided by Dr. Naresh Chandra, Director of BKBCCK, and Dr. Avinash Patil, Principal of BKBCCK, for motivating and facilitating research work in the nanotechnology laboratory.

References

1. Smith et al., 2018, Cobalt oxide nanomaterials for energy applications, *Journal of Materials Chemistry A*, 6(12), 4567–4582.
2. Wang et al., 2019, Co_3O_4 nanoparticles in catalysis, *Applied Catalysis B*, 243(2), 273–285.
3. Liu et al., 2020, Transition metal oxides for supercapacitors, *Electrochimica Acta*, 330(1), 135261–135275.
4. Kumar et al., 2017, Sol–gel synthesis of cobalt oxide nanoparticles, *Ceramics International*, 43(5), 4561–4568.
5. Singh et al., 2016, Green synthesis of metal oxide nanoparticles, *Green Chemistry Letters and Reviews*, 9(4), 345–358.
6. Sharma et al., 2021, Plant mediated synthesis of nanomaterials, *Materials Today Chemistry*, 20(3), 100456–100468.
7. Bilecka & Niederberger, 2010, Microwave chemistry for inorganic nanomaterials, *Nanoscale*, 2(8), 1358–1374.
8. Taguchi et al., 1987, System of Experimental Design, *UNIPUB*, 1(1), 1–45.
9. Roy, 2010, Design of Experiments Using the Taguchi Approach, *Wiley*, 2(1), 55–78.
10. JCPDS Card No. 42-1467, Cobalt oxide (Co_3O_4), International Centre for Diffraction Data.
11. Chen et al., 2015, Structural properties of Co_3O_4 nanoparticles, *Journal of Alloys and Compounds*, 633(4), 138–143.
12. Zhang et al., 2014, Microwave-assisted synthesis of metal oxides, *CrystEngComm*, 16(22), 4850–4861.

13. Patel et al., 2019, Taguchi optimization in nanomaterial synthesis, *Materials Research Express*, 6(9), 0950a1–0950a8.
14. Das et al., 2018, XRD analysis of nanomaterials, *Advanced Powder Technology*, 29(3), 721–729.
15. Ahmed et al., 2022, Green nanotechnology and sustainability, *Environmental Nanotechnology, Monitoring & Management*, 17(1), 100635–100646.

